Mechanical Failure of Fine Root Cortical Cells Initiates Plant Hydraulic Decline during Drought[1][OPEN]

Italo F. Cuneo, Thorsten Knipfer, Craig R. Brodersen, and Andrew J. McElrone*

Department of Viticulture and Enology, University of California, Davis, California 95616 (I.F.C., T.K., A.J.M); School of Agronomy, Pontificia Universidad Católica de Valparaíso, Quillota, Chile (I.F.C.); School of Forestry and Environmental Studies, Yale University, New Haven, Connecticut 06511 (C.R.B.); and USDA-ARS, Crops Pathology and Genetics Research Unit, Davis, California 95616 (A.J.M.)

ORCID IDs: 0000-0002-8092-0987 (I.F.C.); 0000-0001-5945-7273 (T.K.); 0000-0002-0924-2570 (C.R.B.).

Root systems perform the crucial task of absorbing water from the soil to meet the demands of a transpiring canopy. Roots are thought to operate like electrical fuses, which break when carrying an excessive load under conditions of drought stress. Yet the exact site and sequence of this dysfunction in roots remain elusive. Using in vivo x-ray computed microtomography, we found that drought-induced mechanical failure (i.e. lacunae formation) in fine root cortical cells is the initial and primary driver of reduced fine root hydraulic conductivity (Lp_r) under mild to moderate drought stress. Cortical lacunae started forming under mild drought stress (−0.6 MPa Ψ_{stem}), coincided with a dramatic reduction in Lp_r, and preceded root shrinkage or significant xylem embolism. Only under increased drought stress was embolism formation observed in the root xylem, and it appeared first in the fine roots (50% loss of hydraulic conductivity [P_{50}] reached at −1.8 MPa) and then in older, coarse roots (P_{50} = −3.5 MPa). These results suggest that cortical cells in fine roots function like hydraulic fuses that decouple plants from drying soil, thus preserving the hydraulic integrity of the plant's vascular system under early stages of drought stress. Cortical lacunae formation led to permanent structural damage of the root cortex and nonrecoverable Lp_r, pointing to a role in fine root mortality and turnover under drought stress.

Root systems of woody plants consist of both coarse and nonwoody fine roots. Fine roots can constitute as little as 1% of the total root surface area (Kramer and Bullock, 1966), yet are critically important for biogeochemical cycling in terrestrial ecosystems as they constitute the primary exchange surface between plants and soil (Jackson et al., 1997). They are responsible for the vast majority of water absorption in woody root systems (Gambetta et al., 2013; Kramer and Boyer, 1995; Kramer and Bullock, 1966) and mediate backward flow of water from a plant to the soil via a process called hydraulic redistribution, which can alter regional climate (Richards and Caldwell, 1987; Lee et al., 2005). Fine roots also modify the soil through carbon exudation and stimulation of microbial activity (McCormack et al., 2015), and their production and annual turnover represent 33% of global net primary productivity (Jackson et al., 1997; McCormack et al., 2015). Elucidating details of fine root function and responses to stress can thus improve our understanding of how these plant organs can influence ecosystem carbon, nutrient, and water cycles.

Fine roots are traditionally defined as all roots <2-mm diameter, but recent work has emphasized the need to delineate this diameter class into distinct functional groups. By separating fine roots into a shorter-lived absorptive pool and a longer-lived transport pool, McCormack et al. (2015) showed that fine root functionality can alter estimates of global net primary productivity by 30%. This work highlights our still-limited understanding of fine root functionality, the mechanisms underlying their lifespan and turnover, and how those traits respond to abiotic stress (Lukac, 2012; Tierney and Fahey, 2002; Guo et al., 2008). Fine root mortality during drought has been linked to increased root respiration and inhibited photosynthate transport to roots (e.g. Marshall, 1986) but could also be attributed to hydraulic dysfunction (Jackson et al., 2000). Portions of root systems are thought to operate analogously to a hydraulic fuse in an electrical circuit and designed to fail hydraulically when carrying excessive current under drought stress

[1] This work was financially supported by funding from the American Vineyard Foundation to A.J.M. and by USDA-ARS CRIS funding (grant number 5306-21220-004-00). I.F.C. received funding through the Katherine Esau Graduate fellowship program. A.L.S. is supported by the Director, Office of Science, Office of Basic Energy Science, of the U.S. Department of Energy under contract number DE-AC02-05CH11231.

* Address correspondence to ajmcelrone@ucdavis.edu.

The author responsible for distribution of materials integral to the findings presented in this article in accordance with the policy described in the Instructions for Authors (www.plantphysiol.org) is: Andrew J. McElrone (ajmcelrone@ucdavis.edu).

I.F.C., T.K., and A.J.M. designed the experiments and performed the microCT scanning; I.F.C. performed the image analysis; I.F.C. and T.K. performed the root hydraulics and microscopy essays; I.F.C. and A.J.M. wrote the initial draft of the article; T.K. and C.R.B. revised and edited the article; C.R.B. and A.J.M. obtained funding and microCT beamtime; A.J.M. supervised the project.

[OPEN] Articles can be viewed without a subscription.

www.plantphysiol.org/cgi/doi/10.1104/pp.16.00923

(Zimmermann, 1983; Jackson et al., 2000). However, the exact location of these hydraulic fuses in the root system has yet to be identified. Axial water transport in the xylem is considered a weak link, as roots of numerous species have been shown to be more susceptible to drought-induced xylem embolism compared to other organs within the same plant (i.e. trunks, stems, tap roots; Alder et al., 1996; Hacke and Sauter, 1996; McElrone et al., 2004; Pratt et al., 2015; Johnson et al., 2016). Moreover, Sperry and Ikeda (1997) found that smaller roots were the most vulnerable plant organ to xylem embolism, which would localize failure to inexpensive, distal, and easily replaceable portions of a root system. Such a design is considered effective, because it is widely assumed that the hydraulic capacity of smaller distal roots is readily repaired upon rewatering via xylem embolism removal (Domec et al., 2006; Jackson et al., 2000). While much work has demonstrated that xylem embolism reduces hydraulic capacity under severe drought stress (Brodribb et al., 2016a, 2016b; Choat et al., 2012), its contribution under mild to moderate stress is less clear (Choat et al., 2016; Cochard and Delzon, 2013; Cochard et al., 2013; McElrone et al., 2012; Wheeler et al., 2013; Choat et al., 2010; Torres-Ruiz et al., 2015). Work is still needed to resolve the location and sequence of root hydraulic dysfunction under drought and what tissues are involved in each stage of this process, especially under mild stress where fine root hydraulic conductivity (Lp_r) is known to decrease dramatically (Aroca et al., 2012).

Before entering the xylem for long distance transport, water absorbed by roots must traverse a series of cell layers that include the epidermis, cortex, and endodermis (Steudle and Peterson 1998). Hydraulic resistance is much greater along this radial pathway compared to the axial transport pathway in the xylem (e.g. Frensch and Hsiao, 1993; Frensch and Steudle, 1989). The resistance differential between radial and axial pathways persists or increases in magnitude as fine Lp_r decreases under mild to moderate drought stress. While decreased fine root permeability under drought has been attributed to root shrinkage (Passioura, 1988; Nobel and Cui, 1992), changes in membrane permeability via aquaporins (Maurel et al., 2015; Aroca et al., 2012; North, 2004), development of suberized apoplastic barriers over longer periods of drought (Barrios-Masias et al., 2015; North and Nobel, 1991), or mechanical damage in cortical cells (i.e. lacunae formation; North and Nobel, 1991), the integration of these responses particularly under mild stress is still lacking. Elucidating the physiological mechanism that drives this response could help to resolve long-standing questions about fine root functionality, lifespan, and turnover.

Here, we originally aimed to study whether fine roots function as the primary hydraulic fuse that disconnects a plant from drying soil. We studied the sequence of events during soil drying from saturated to severe drought conditions in coarse and fine roots of grapevines, which are considered a model species and have long been characterized as highly susceptible to drought-induced embolism. While performing these experiments, we discovered that the fine root cortex was radically changing under mild drought stress that preceded any embolism formation. We then performed hydraulic measurements and fluorescence light microscopy to investigate how fine Lp_r is affected by the formation of cortical lacunae that should significantly increase radial hydraulic resistance to flow.

RESULTS

In Vivo Observation of Changes in Root Structure and Function

We used noninvasive, x-ray microtomography (microCT) imaging to visualize the functional status of fine and coarse roots on grapevines subjected to a range of drought stress. The plants were exposed to a range of drought severity conditions from fully saturated to extremely dry soil, which approximated the full spectrum of soil water availability for grapevines growing in natural and agricultural settings. In fully saturated soil, fine and coarse roots were well hydrated, with the tissues intact and the majority of the xylem fully functional (Fig. 1, A and B). As the soil dried, we observed the formation of cortical lacunae in fine roots but not in coarse roots (-0.6 MPa stem water potential [Ψ_{stem}]; Fig. 1, A and B). The cross-sectional area created by cortical lacunae increased with drought stress severity and reached a maximum of 30.6% of the cortex at -1.2 MPa Ψ_{stem} (Fig. 1B). Beyond this point (i.e. -1.7 MPa Ψ_{stem} in Fig. 1B), severe stress led to the collapse of cortical lacunae. In coarse roots (Fig. 1A), there was no formation of cortical lacunae at any level of stress. Cortical lacunae also formed when roots were subjected to increasingly osmotic solutions; the threshold of cortical lacunae initiation was at -0.5 MPa Ψ_{stem} (Fig. 2). Importantly, cortical lacunae did not occur in the range of osmotic potential (Ψ_π) of sucrose solutions used in the hydraulic experiment.

Three-dimensional volume renderings of fine roots revealed the spatial organization and physical structure cortical lacunae otherwise difficult to observe with typical microscopic techniques (Fig. 3). The formation of cortical lacunae is followed by the disruption of the cell wall (Fig. 3, A and B). Structurally, cortical lacunae formed air-filled channels along the root axis (Fig. 3, A1 and A2). Lacunae formation occurred mainly in the central cell layers of the cortex, thereby decoupling the tissue immediately surrounding the epidermis and the xylem and disrupting the radial hydraulic pathway (Fig. 3, A and B). This region contained the largest cortical cells with a mean diameter of 79 μm ($\pm$ 4 μm SE), while cortical cells in the outer and inner layers had mean diameters of 41 μm ($\pm$1 μm SE) and 46 μm ($\pm$2 μm SE), respectively (Supplemental Fig. S1).

Embolism formation was minimal or nonexistent for both root classes under well-watered conditions (i.e. Ψ_{stem} ranging between -0.3 and -0.5 MPa) and started increasing with more negative Ψ_{stem} (Figs. 1, A and B, 4).

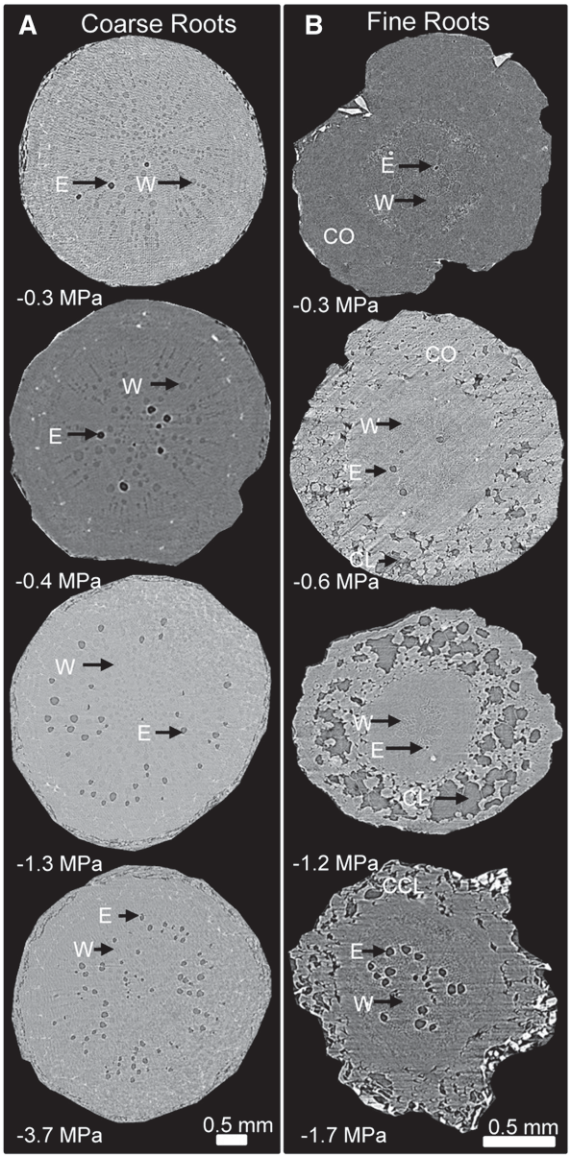

Figure 1. Transverse microCT images through fine and coarse roots of grapevine showing embolism and cortical lacunae at different Ψ_{stem}. E, embolized vessels (dark gray color); W, water-filled vessels (light gray color); CO, cortex; CL, cortical lacunae; CCL, collapsed cortical lacunae.

Fine roots were more susceptible to embolism formation and reached predicted 50% loss of hydraulic conductivity (P_{50}) at −1.8 MPa Ψ_{stem}, whereas coarse roots reached the predicted P_{50} at −3.5 MPa Ψ_{stem} (Fig. 4). Because vessel diameter is often correlated with xylem vulnerability to cavitation (McCulloh et al., 2012), we measured vessel diameter distributions of all vessels in the two root classes as well as the diameter of embolized and water-filled vessels in vivo. Vessel diameters were larger in coarse, woody roots compared to fine roots (42% of fine root vessels were 20–40 μm in diameter, while 43% of coarse root vessels were 40–60 μm in diameter; Supplemental Fig. S2). The mean diameter of embolized vessels was significantly, and unexpectedly, smaller than water-filled vessels for fine and woody roots (Supplemental Fig, S2, inset).

Changes in Hydraulic Properties

To test the physiological significance of cortical lacunae formation, we measured Lp_r and found that Lp_r decreased >50% at the same water potentials that induced cortical lacunae formation and no xylem embolism (−0.6 MPa; Fig. 5). The percentage of cortical lacunae in the cortex increased in the same region of drought stress where the decay in hydraulic conductivity occurred, reaching a maximum of 31% at Ψ_{stem} of −1.1 MPa (Fig. 5). In this experiment, we observed no recovery of Lp_r in fine roots subjected to drought stress ranging from −1.0 to −2.0 MPa Ψ_{stem} (Fig. 5), while the Ψ_{stem} recovered to initial conditions observed in well-watered plants in fully saturated soil (i.e. approximately −0.5 Mpa; Fig. 5). Similarly, stomatal conductance showed a reduction of approximately 74% during the dry-down (i.e. at −1.1 Ψ_{stem}) and recovered to approximately 70% of the total (i.e. stomatal conductance of well-watered plants at the beginning of the experiment) after 1 d of rewatering (Supplemental Fig. S3).

We then used fluorescence microscopy to detect the degree of suberin and lignin deposition in the cross-sectional area of coarse and fine roots. There was no visible difference in suberin-lignin deposition between well-watered and drought-stressed plants at different locations along the root (Supplemental Fig. S4).

DISCUSSION

Our results provide evidence from in vivo imaging that abrupt decreases in Lp_r under drought are directly linked to structural damage to fine root cortical cells via lacunae formation. Previous work has attributed the loss of hydraulic capacity of drought-stressed root systems to xylem embolism formation (McElrone et al., 2004; Pratt et al., 2015) and/or root shrinkage (Nobel and Cui, 1992; North and Nobel, 1997). Here, both embolism and tissue shrinkage lagged well behind lacunae formation. These results suggest that cortical tissue in fine roots act as a very vulnerable link in the water transport pathway, which may help to explain fine root lifespan/turnover and changes in ecosystem fluxes under drought stress.

At a whole-plant level, it is reasonable to think that a potential hydraulic fuse might be located in distal tissues in the canopy, where Ψ is most negative (i.e. in the leaves). Dry and warm atmospheric conditions would push leaves beyond a water potential threshold and trip the hydraulic fuse in the leaf or petiole, thereby preventing both excessive water losses to the atmosphere and the buildup of hydrostatic tension in the xylem that would lead to systemic and catastrophic embolism spread (McCulloh and Woodruff, 2012; Tyree et al., 1993; Zimmermann, 1983). However, root xylem has been

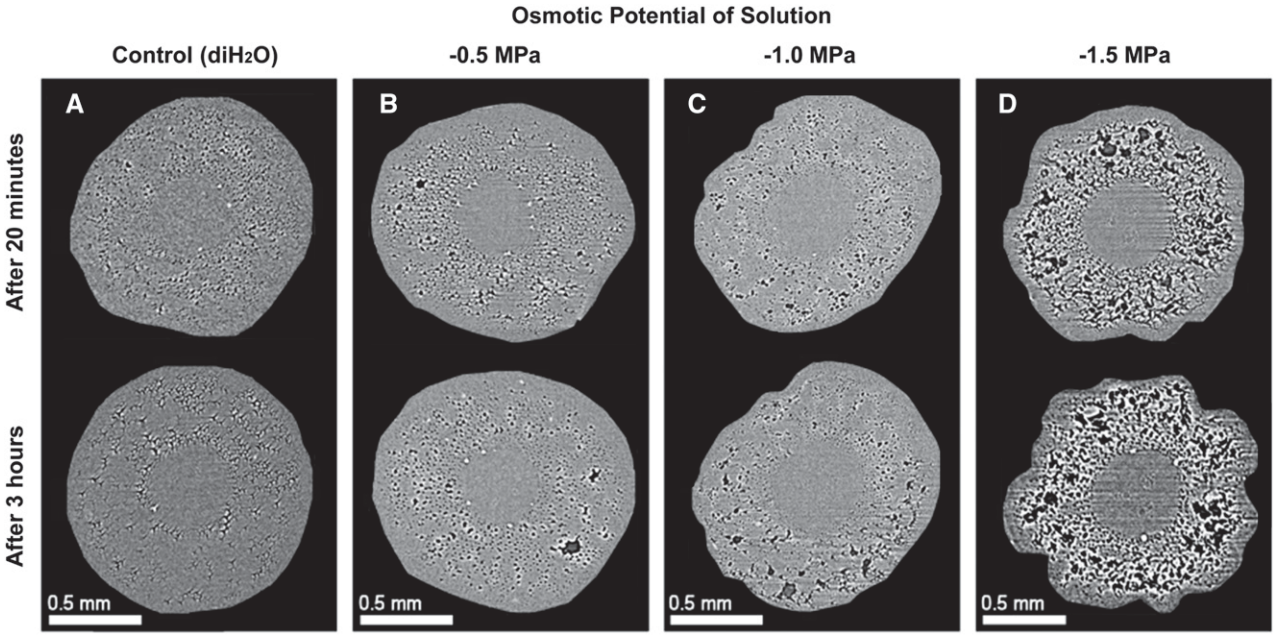

Figure 2. Cortical lacunae formation over time induced by using sucrose solutions with Ψ_π of 0, −0.5, −1.0, and −1.5 MPa. A, Roots subjected to diH20 (control) showed no cortical lacunae formation after 3 h. B and C, Roots subjected to solutions with osmotic potentials of −0.5 and −1.0 MPa showed initiation of cortical lacunae after 3 h. D, Roots immersed in −1.5 MPa osmotic potential solutions showed the highest cortical lacunae formation after 3 h.

reported to be more vulnerable to embolism formation than shoot xylem in many woody plants (McElrone et al., 2004; Alder et al., 1996; Sperry et al., 1998; Kolb and Sperry, 1999; Ewers et al., 2000; Hacke et al., 2000; Hacke, 2000; Pratt et al., 2015). While we found that the xylem of fine roots was more susceptible to drought-induced embolism compared to coarse roots, which agrees with previous findings (Sperry and Ikeda, 1997), our current work highlights that the weakest link in the soil-plant-atmosphere continuum is in an even more distal tissue, yet still within the plant body. Furthermore, while isolating the hydraulic fuse inside the cortex, the tissue damage would be restricted to internal structures and preserve the critical barrier formed by the epidermis (Fig. 6). Even though cortical lacunae in fine roots can be interpreted as a kind of hydraulic fuse, our data show that Lp_r does not drop to zero. Instead, lacunae might be more appropriately understood as a variable resistor in the radial pathway, limiting both water uptake capacity and outward flow back in to drying soils when Ψ_{soil} is more negative than Ψ_{root} (Nobel and Sanderson, 1984; Schulze et al., 1998). To reestablish the hydraulic properties of fine roots, growth of new laterals or/and regrowth from the distal meristem would be needed (Jackson et al., 2000).

Cortical lacunae have been documented exclusively in monocots (Esau, 1965; Stasovski and Peterson, 1991) or desert succulents (North and Nobel, 1991, 1992, 1997). They are thought to form readily in grasses from relatively dry habitats (Beckel, 1956) and are known to form in desert succulents under conditions of drying soil (North and Nobel, 1991). To our knowledge, results presented here are the first documentation of these structures in a plant that occupies more mesic habitats; grapevines, including those native to arid regions of the southwest US, are typically found growing in proximity to water sources. Root cortical lacunae can appear similar to aerenchyma but form as a result of extensive breakdown of cells by processes of lysigeny (i.e. the creation of cavities by lysis) or rhexigeny (i.e. the spontaneous mechanical rupture of cells; Esau, 1965). Lysigenous or rhexigenous intercellular air spaces are both bound by broken walls (unlike aerenchyma) and have irregular shapes and distributions (Esau, 1965). We suspect that the cortical lacunae form in grapevine roots by rhexigeny, but further study is needed to determine the exact processes involved. It is interesting to note that these form in the same region of the fine root cortex, where one might expect aerenchyma to form. Aerenchyma are known to form in roots subjected to hypoxic and water-logged conditions (Drew et al., 2000), and given that grapevines are native to riparian habitats, cortical cells in the fine roots may be predisposed to mechanical failure under drought stress because these cells have a tendency to form aerenchyma.

Cortical lacunae formation in succulent plants was linked to a drop in Lp_r by approximately 50% per day after the dry-down was initiated, and cortical lacunae were estimated to occupy 24% of the cortex after 7 d of drought (North and Nobel, 1991, 1992). Lp_r recovered almost completely in young fine roots (North and Nobel, 1991, 1992) after 7 d of rewetting. We found no recovery of Lp_r 24 h after rewatering even though the

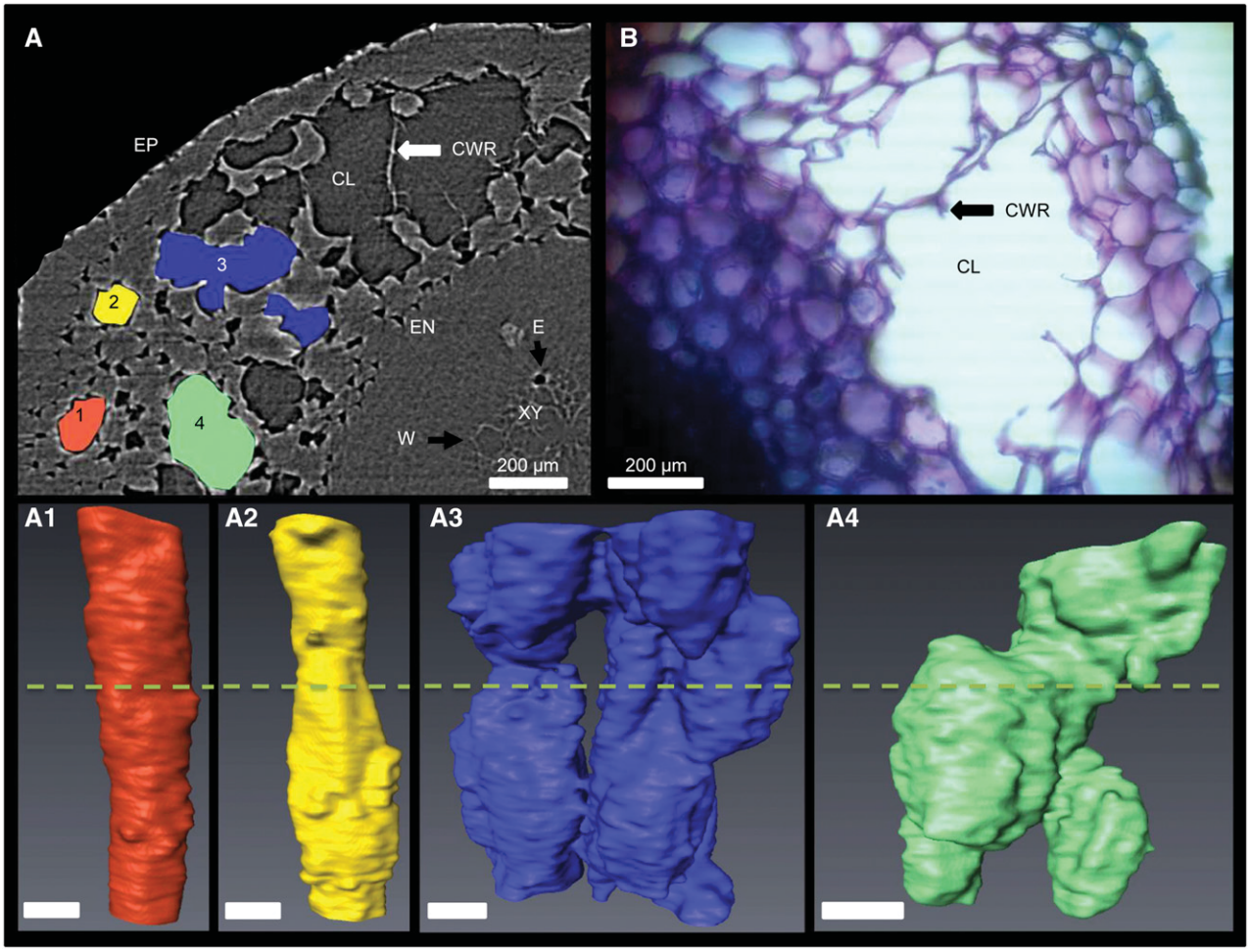

Figure 3. Typical examples of the spatial structure of drought-induced cortical lacunae in grapevine fine roots. A, Transverse microCT image showing the area covered by cortical lacunae in fine roots, and corresponding volume renderings (A1, 2, 3, 4) showing the 3-D shape of cortical lacunae in A. Dashed line corresponds to the approximate position of transverse microCT image from A. B, Example of a free-hand cross-section of a fine root showing cortical lacunae and cell wall remnants, similar to observation using microCT imaging. E, Embolized vessels (dark gray color); W, water-filled vessels (light gray color); CL, cortical lacunae; CWR, cell wall remnant; EP, epidermis; EN, endodermis; XY, xylem. Bars = 50 μm (when not specified).

Ψ_{stem} did recover (Fig. 5). This recovery in water potentials might be explained by water uptake through root regions with no lacunae formation (i.e. not damaged tissue in fine roots or through coarse roots) or through the remaining but limited cell wall material (i.e. residual apoplastic pathway) in these fine roots. Given the disruption of cortical cells that occurs during lacunae formation, it is surprising that previous work found that Lp_r would recover upon rewatering, since most water moves through the apoplastic pathway. Such a response may depend on the method used to evaluate hydraulic conductivity of the root tissue. For example, if positive hydrostatic pressure is used to drive flow through the tissue after lacunae form, it is likely that these voids would be filled with water and much of the resistance along the radial pathway removed. If this happens, fine root Lp_r would actually appear the same or greater after drought, hiding the fact that the absorptive tissue is not actually functional. In this study, we used osmotic gradients to evaluate changes in Lp_r associated with lacunae formation to avoid potential artifacts with these measurements.

Here, we propose a conceptual model that relates cortical lacunae formation with fine root turnover (Fig. 6). Fine roots under well-watered conditions exhibit intact apoplastic and cell to cell pathways (Fig. 6), but when they experience a mild level of stress (i.e. $\Psi_{stem} = -0.6$ MPa), they start showing signs of cell shrinkage and tearing/breakdown and the radial pathway start being severely affected (i.e. Lp_r start decaying exponentially; Fig. 6). At this point, embolism formation is not a limitation for water transport. When $\Psi_{stem} = -1.2$ MPa, large lacunae that originated from initial cell breakdown coalesce and occupy a maximum of approximately 30% of the cortex and the radial pathway is limited (Fig. 6). The

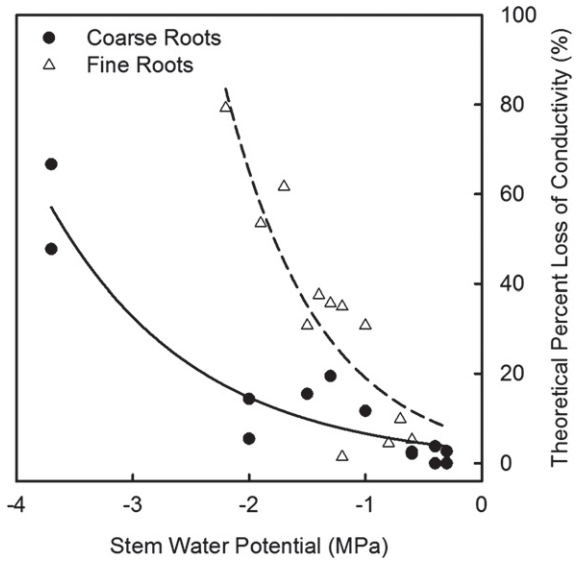

Figure 4. Theoretical percent loss of conductivity for grapevine fine and coarse roots; values were calculated using the diameter of embolized and water-filled vessels. For fine roots, data were best fitted with an exponential function (dashed line; $y = 5.5745e^{(-1.23x)}$, $R^2 = 0.81$, $P < 0.0001$). For coarse roots, data were best fitted with an exponential function (solid line; $y = 2.9924e^{(-0.7967x)}$, $R^2 = 0.90$, $P < 0.0001$).

roots that reach this point experience unrecoverable reductions in hydraulic transport capacity, and the severe disruption of cortical cells would cause cellular contents to float around freely in the tissue. The consequences for such a release of contents and whether they become a substrate for microbial contamination (i.e. pathogen) or serve as a release of carbon to the soil remain unanswered. Under extreme drought conditions for grapevines (i.e. $\Psi_{stem} = -1.7$ MPa), the fragile cortical structure containing lacunae collapse and root shrinkage happen (Fig. 6). At this point, the cortex of the root is severely damaged, and embolism in the xylem starts being a relevant limitation to water transport (P_{50} is reached). Based on the severe damage and permanent loss of functionality, we speculate that root turnover is inevitable under mild drought conditions in the field. Future work is needed to elucidate the fate of the apical meristem and formation of lateral roots after a drought event.

In this study, we used Ψ_{Stem} as a proxy for water stress in our potted plants. Predawn water potential (Ψ_{PD}) measurements are often used to estimate soil water potentials, and it can be argued that this would better reflect the conditions that would induce cortical lacunae. According to classical water relations theory, predawn plant water status is expected to equilibrate with the wettest soil layer in the rooting zone overnight, and thus Ψ_{PD} measurements can be a good approximation of soil water status experienced by fine roots assuming sufficient time for the plant to equilibrate, limited nighttime transpiration, and/or limited internal hydraulic resistances or capacitance within the plant (Donovan et al., 1999). In our small experimental plants, Ψ_{Stem} functions as a reasonable estimate of the stress experienced by the entire plant (i.e. it faithfully represents the stress imposed by a drying soil), because the soil water potential dropped rapidly in concert with decreases throughout the plant (Supplemental Fig. S3), but water potential gradients can be much larger in mature field-grown plants. Under field conditions, our findings likely translate most closely to young, recently established vines but have implications for mature plants as well. Numerous studies have documented Ψ_{PD} between −0.5 and −1.1 MPa for field-grown grapevines subjected to drought conditions (Centeno et al., 2010; Williams and Baeza, 2007; Intrigliolo and Castel, 2006; Williams and Araujo, 2002; Choné et al., 2001). How readily lacuna will form under field conditions will depend on a variety of conditions that impact the rate at which the soil dries under deficit conditions. On a daily basis, a mature and well-watered grapevine can experience midday Ψ_{Stem} ranging from −0.7 to −1.0 MPa (Centeno et al., 2010; Williams and Araujo, 2002; Choné et al., 2001). Based on our findings using Ψ_{Stem} as our stress proxy, one might expect that the roots are forming lacuna even under well-watered conditions. However, during the initial stages of soil drying following an irrigation or precipitation event, the Ψ_{PD} will typically be in the range of −0.1 to −0.3 MPa (Williams et al., 2012). As the soil dries, the Ψ_{PD} of the plant begins to drop and will

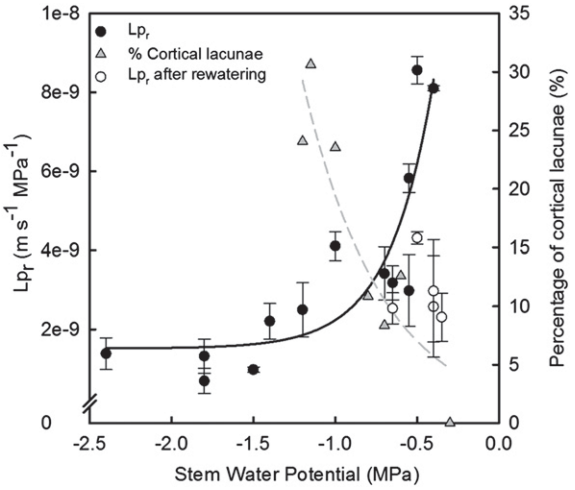

Figure 5. Drought-induced changes in Lp_r and percentage area covered by cortical lacunae (of total cortical area) in grapevine fine roots as a function of stem water potential. Each gray triangle symbol represents a single root analyzed (dashed gray line is best fit, $y = 2.5319e^{(-2.0396x)}$, $R^2 = 0.84$, $P = 0.0035$). Lp_r was measured on roots obtained from plants subjected to drought at different Ψ_{stem} (solid line is best fit, $y = 1.5166^{-9} + 3.0421^{-8}e^{(3.7435x)}$, $R^2 = 0.72$, $P < 0.0001$). To evaluate the ability to recover Lpr following drought, Lp_r was determined from rewatered plants. (i.e. in the region of Ψ_{stem} between −1.0 and −2.0 MPa) that recovered for 1 day after watering. Each circle represents mean ± SE ($n = 3$ roots).

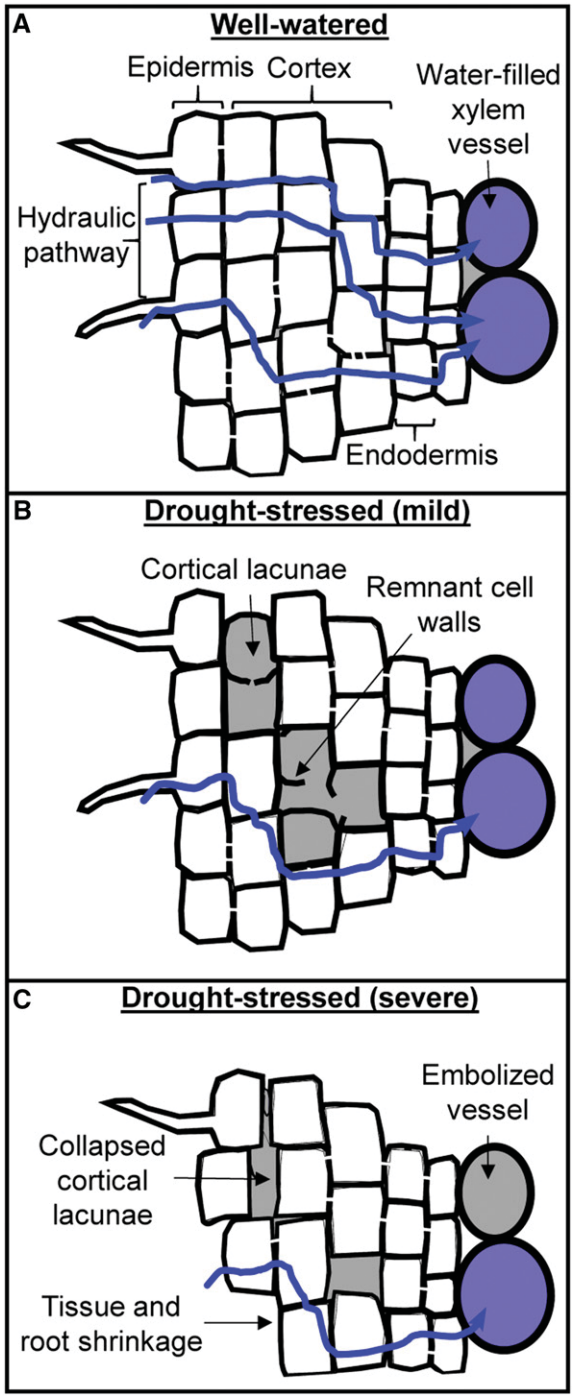

Figure 6. Schematic illustration of cortical lacunae progression and its implications on Lp_r. A, Root of a well-watered plant showing no sign of strain. B, Cortical lacunae develop via cell death (rhexigeny) and the radial hydraulic properties are severely affected. C, Cortical lacunae collapses causing root shrinkage, and xylem embolism starts being relevant.

enter the range at which lacuna formation can occur; various studies have documented Ψ_{PD} values of −0.5 to −1.1 MPa in grapevines that depend on the duration of a drought event (intermittency of irrigation), soil type, climate, variety, etc. At this point, more work is needed to resolve how our current findings translate to field grown plants, especially since water relations theory assumes that plants will come into equilibrium with the wettest portion of the soil. In growing situations with large soil resource heterogeneity (e.g. in irrigated agricultural systems where drip emitters create highly uneven water distributions), lacunae formation is likely to occur earlier in drier patches and is likely effective by soil types or soil drying over sufficient time. The experimental design in this manuscript suggest that drying soils are the primary trigger of this cellular dysfunction, similar to findings of North and Nobel (1991) where the appearance of cortical lacunae and its effects on Lpr in drying soils developed over time. This is further reinforced by our experiment utilizing external sugar solutions to induce lacunae formation. However, future work is needed to elucidate if lacunae formation is a response of a combination of drying soils and a build-up of tensions in the xylem.

These data provide a detailed visualization of the initial conditions experienced by fine and coarse roots in a drying soil highlighting the dynamics of the breakdown of both the radial and axial hydraulic pathways. Though this process is described here for only grapevine, this agriculturally important crop species serves as a model system for understanding the physiology of woody plants. Establishing this method of fine root visualization in grapevine is an important first step and should be followed by the investigation of fine roots in other species to partition the variable resistances of whole Lp_r. Our data also underscore the importance of the functional distinction of fine roots in the context of ecosystem modeling of fine root turnover. Our data suggest that an absorptive fine root subjected to drought and showing cortical lacunae formation will experience a dramatic loss of absorptive functionality, and any classification in the absorptive group will necessarily be flawed. However, an improved classification system of fine roots by both functional and structural traits could help to better understand fine root turnover and lifespan (Green et al., 2005; Hendrick and Pregitzer, 1996; Baddeley and Watson, 2005; Mainiero and Kazda, 2006). Our results also show that hydraulic dysfunction in the cortex of fine roots under even mild stress would be particularly important for agricultural plants where maximizing carbon capture is critical, and even mild soil drying could result in significant declines in water transport, increases in carbon investment for fine root turnover, and therefore net carbon loss resulting from inadequate water availability. Collectively, these data and future work on additional species will serve to better represent the radial and axial pathways in root network models as well as the soil conditions that would initiate the turnover of one of the principle components of global net primary productivity.

MATERIALS AND METHODS

Plant Material

Herbaceous cuttings of grapevine rootstock Ruggeri 140 (140 RU; *Vitis berlandieri X v rupestris*) were collected at the University of California, Davis, experimental vineyards. The basal node of each cutting was soaked in 2.5% rooting solution (Earth Science Products), placed in a plastic tray filled with growing medium (50% vermiculite, 50% perlite), and maintained for 15 d in a mist room until there were signs of root initiation and growth (Knipfer et al., 2015). To obtain access to coarse roots for microCT analysis, cuttings were fixed to the top of a plastic cylinder (length 35 mm, diameter 8 mm) filled with sand such that coarse roots developed along the tube, and the bottom 2 cm of the cylinder was inserted in a 1.4-L plastic pot filled with sand that allowed root system expansion (Supplemental Fig. S5A for set-up). For microCT analysis of fine roots, cuttings were transplanted into 0.2-L plastic cups filled with sand for root system growth, and a plastic tube of 20 cm long filled with sand connected to the bottom of the plastic pot allowed fine roots to develop while facilitating the access to the target zone (Supplemental Fig. S5B for set-up). Plant growth was maintained under environmental controlled conditions (approximately 15°C to 25°C temperature, 35% relative humidity, 500–600 μmol photons m^{-2} s^{-1}, and 16-h-ligh/8-h-dark cycle), and hydrated via drip irrigation three times a day with water supplemented with macro- and micronutrients (Gambetta et al., 2013). To induce water stress, irrigation was removed up to 3 d prior the experiment. At the moment of the measurement, plants had at least one shoot of approximately 30 cm long with 8 to 12 leaves.

For hydraulic measurements and fluorescent microscopy experiments, plants were grown in 1.1-L plastic pots filled with sand under similar growth conditions (see above).

Measurements of Plant Water Status

Ψ_{stem} of plants was measured using a Scholander pressure chamber (Soil Moisture Equipment Corp. 3005). Mature leaves were placed into aluminum bags for at least 15 min such that they were hydraulically equilibrated with Ψ_{stem}. Subsequently, leaves were excised in the base of the petiole and placed into the pressure chamber. The chamber was pressurized, and the pressure required to force water out of the petiole base was recorded and defined as Ψ_{stem}.

microCT

In vivo imaging of plant tissue was performed at the Advance Light Source (ALS) Lawrence Berkeley National Laboratory, beamline 8.3.2. Plants were transported from UC Davis campus to ALS by car and imaged within <24 h. Prior to imaging Ψ_{stem} was measured. Plants were mounted in the microCT beamline as follows. For coarse root set-up, each plant analyzed (n = 12, range in Ψ_{stem} of 0.3 to −3.7 MPa), the plastic cylinder and sand medium surrounding coarse roots was carefully removed, and the plastic pot was placed in an aluminum cage and fixed on an air-bearing stage (Supplemental Fig. S5A; Brodersen et al., 2010; McElrone et al., 2013; Knipfer et al., 2015). For fine root set-up, in each plant analyzed (n = 12, range in Ψ_{stem} of −0.3 to −1.7 MPa), the lower portion of the plastic cylinder with sand medium surrounding fine roots was carefully removed, the excavated fine roots were inserted into a plastic tube (length 15 cm) that was fixed to the remaining upper portion of the remaining plastic cylinder, and the plastic tube was inserted into the drill chuck and then placed on the stage (Supplemental Fig. SB). Due to the high density of sand particles and their high x-ray absorption, it was necessary to remove the sand surrounding the roots prior to imaging. Roots were subjected to a single scan to eliminate possible measuring artifacts induced by x-ray exposure. For microCT imaging, an 18-keV synchrotron x-ray beam was used. During scanning, the sample was rotating continuously, and 1,024 longitudinal images per 180° rotation were collected using a 4008- x 2672-pixel CCD camera (PCO 4000, Cooke Corporation) at a 200-s exposure time. The resolution of images was 4.5 μm/pixel (coarse roots) and 1.8 μm/pixel to 0.9 μm/pixel (fine roots). The acquired images were reconstructed into a stack of transverse images using Octopus 8.3 software (Institute for Nuclear Sciences), a custom plug-in for Fiji imaging-processing software (www.fiji.sc, ImageJ).

To test if osmotic stress, similar to drought stress, could impose structural changes to the root tissue, some fine roots of well-watered plants were excised, the open end of the root was sealed with petroleum jelly and wax tape (Parafilm M), and the root was submerged in sucrose solutions of 0, −0.5, −1.0, and −1.5 MPa of osmotic potential (Ψ_π). The range of Ψ_π was selected to be in the range of Ψ_{stem} of drought-stressed plants. Subsequently fine roots were scanned after 20 min and 3 h.

MicroCT Image Analysis

Embolized and water-filled vessels were determined from transverse microCT image slices. Using a semiautomated routine in Fiji (Schindelin et al., 2012; as described in Brodersen et al., 2013), vessel number and cross-sectional area (A) were determined by using the Analyze Particles tool. Vessel diameter (d) was derived by $A = \pi(d/2)^2$. Percentage theoretical loss of xylem hydraulic conductivity was determined using a modified Hagen-Poiseuille equation (Tyree and Ewers, 1991; Brodersen et al., 2013; Knipfer et al., 2015). The xylem hydraulic conductivity (k_h) of the population of embolized and water-filled vessels of the roots was calculated according to:

$$k_h = \frac{\pi\rho}{128\mu} \sum_{i=1}^{n}(d_i^4),$$

where d corresponds to vessel diameter, ρ is the density of the fluid in Kg m^{-3}, and μ is the viscosity of water in MPa s. Maximum hydraulic conductivity (k_{max}) was calculated by $k_{embolized} + k_{h(water\text{-}filled)}$. Consequently, theoretical percentage loss of xylem hydraulic conductivity was calculated according to:

$$PLC = \left(1 - \frac{k_h}{k_{max}}\right) * 100.$$

Percentage of air-filled tissue in the root cortex by cortical lacunae was obtained by using the Analyze Particles tool in Fiji (Schindelin et al., 2012). The total area of the cortex was obtained by subtracting the area between the endodermis and the center of the root to the area between the epidermis and the center of the root. The percentage of cortical lacunae was calculated by [(area of cortical lacunae/total area of cortex) *100%].

The frequency distribution of vessel diameters was generated from a population of 1,745 vessels from fine roots (n = 12) and woody roots (n = 12). First, diameter classes of 20 μm (i.e. 0–20 μm, 20–40 μm, etc.) were created arbitrarily. Vessel diameters were categorized and frequency per class was determined by frequency (%) = [(number of vessels per diameter class/total number of vessels) *100%]. Each class was then averaged across the roots analyzed separately for fine and woody roots.

Lp_r

Plants were transported from the greenhouse to the laboratory, where Ψ_{stem} was measured immediately. The root system was carefully removed from the pot, and fine roots were excised under water at approximately 10 cm from the tip. Lp_r was measured osmotically (Gambetta et al., 2012) to prevent the collapsing of potential air-spaces in the root tissue that may have formed under drought, as would be the case by pressuring the root to obtain a hydrostatic Lp_r (Barrios-Masias et al., 2015). The proximal-open end of the root was connected to a glass microcapillary (0.25-mm i.d.; Stoelting) and the connection was sealed with superglue (Loctite gel; Henkel). The microcapillary was half-filled with diH_2O, and the roots were subjected to sucrose solutions of 0, −0.14, and −0.32 MPa. Each osmotic pressure step was applied in a downward order for 20 min, and the displacement of the meniscus was tracked every 5 min. The −0.32 MPa osmotic pressure step was applied twice to check how flow was compared to the initial measurement. Changes in volume (V) were obtained for each pressure step by

$$Volume = \pi(r^2)d,$$

where r is the radius of the microcapillary and d corresponds to the distance traveled by the meniscus. Because water flow directionality was different depending on the osmotic pressure step (i.e. inward the root for 0 MPa and outward the root for −0.32 MPa), a negative sign (−) was assigned to volumes with outward directionality and a positive (+) was assigned to volumes with inward directionality (Supplemental Fig. S6). Then, volumetric flow rate (Q; m^3 s^{-1}) was calculated as the slope of the linear regression line between the cumulative volume (m^3) and cumulative time (s). A second linear regression line was fitted between Q and the osmotic pressure gradient (ΔP), and the slope of this line represented hydraulic conductance (C; m^3 s^{-1} MPa^{-1}). The surface area (A; m^2) of the root was measured by using winRhizo (WinRhizo Pro 2009b, Régent Instruments), and Lp_r (m s^{-1} MPa^{-1}) was calculated by $Lp_r = C/A$.

Fluorescent Light Microscopy

Free-hand cross-sections of roots were performed with fresh razor blades at two different regions (i.e. 2–4 and 12–14 cm from root tip). Roots were stained with 0.1% (w/v) berberine-hemisulfate for 1 h, rinsed with water, and stained for 30 min with toluidine blue (Brundrett et al., 1988; Barrios-Masias et al., 2015;

Gambetta et al., 2013). The stained sections were mounted on a slide with diH_2O and observed under violet fluorescence light (excitation filter, 400- to 410-nm peak emission; dichromatic mirror, 455 nm; and barrier filter, 455 nm) using an Olympus Vanox-AHBT (Olympus America) compound microscope. Images were acquired with a 600ES digital camera (Pixera). Suberin-lignin in the exodermis and endodermis appeared bright yellow (Brundrett et al., 1988; Barrios-Masias et al., 2015).

Leaf Gas Exchange

Stomatal conductance was measured midday between 11:00 and 13:00 h in the greenhouse using a SC-1 leaf porometer (Decagon Devices). Three mature and healthy leaves were selected on each plant and treated as subsamples. Each leaf of each plant was repeatedly measured for well-watered, drought-stressed, and rewatered (after 1 d) conditions. There was no sign of necrosis or leaf dieback in response to drought during the dry-down. At the same time, predawn and midday stem water potentials were measured in the same plants. The plant material, growing conditions, and imposed drought stress used in this experiment were the same as in other experiments used here.

Supplemental Data

The following supplemental materials are available online.

Supplemental Figure S1. Mean diameter of cells located in the outer, middle, and inner layers of the cortex.

Supplemental Figure S2. Frequency distribution of all vessel diameters in fine and coarse roots.

Supplemental Figure S3. Free-hand cross-sections of fine roots obtained from grapevine plants subjected to well-watered and drought-stress conditions.

Supplemental Figure S4. Predawn and midday stem water potentials (a) and stomatal conductance (b) measurements of well-watered, drought-stressed, and rewatered (after 1 d) plants.

Supplemental Figure S5. Cartoon illustrating how plants were grown in order to get access to coarse and fine roots.

Supplemental Figure S6. Representative relationship between osmotic pressure and volumetric flow rate.

ACKNOWLEDGMENTS

The authors kindly thank D. Parkinson and A. MacDowell for their assistance at the Lawrence Berkeley National Laboratory ALS Beamline 8.3.2 microtomography facility. Thanks also to C. Albuquerque, J. Uretsky, P. Lenain, and P. Terrassa for help with plant preparation.

Received June 8, 2016; accepted September 8, 2016; published September 12, 2016.

LITERATURE CITED

Alder NN, Sperry JS, Pockman WT (1996) Root and stem xylem embolism, stomatal conductance, and leaf turgor in *Acer grandidentatum* populations along a soil moisture gradient. Oecologia **105:** 293–301

Aroca R, Porcel R, Ruiz-Lozano JM (2012) Regulation of root water uptake under abiotic stress conditions. J Exp Bot **63:** 43–57

Baddeley JA, Watson CA (2005) Influences of root diameter, tree age, soil depth and season on fine root survivorship in *Prunus avium.* Plant Soil **276:** 15–22

Barrios-Masias FH, Knipfer T, McElrone AJ (2015) Differential responses of grapevine rootstocks to water stress are associated with adjustments in fine root hydraulic physiology and suberization. J Exp Bot **66:** 6069–6078

Beckel DKB (1956) Cortical disintegration in the roots of *Bouteloua gracilis* (H. B. K) LAG. New Phytol **55:** 183–190

Brodersen CR, McElrone AJ, Choat B, Lee EF, Shackel KA, Matthews MA (2013) In vivo visualizations of drought-induced embolism spread in *Vitis vinifera.* Plant Physiol **161:** 1820–1829

Brodersen CR, McElrone AJ, Choat B, Matthews MA, Shackel KA (2010) The dynamics of embolism repair in xylem: in vivo visualizations using high-resolution computed tomography. Plant Physiol **154:** 1088–1095

Brodribb TJ, Bienaimé D, Marmottant P (2016a) Revealing catastrophic failure of leaf networks under stress. Proc Natl Acad Sci USA **113:** 4865–4869

Brodribb TJ, Skelton RP, McAdam SA, Bienaimé D, Lucani CJ, Marmottant P (2016b) Visual quantification of embolism reveals leaf vulnerability to hydraulic failure. New Phytol **209:** 1403–1409

Brundrett MC, Enstone DE, Peterson CA (1988) A berberine-aniline blue fluorescent staining procedure for suberin, lignin, and callose in plant tissue. Protoplasma **146:** 133–142

Centeno A, Baeza P, Lissarrague JR (2010) Relationship between soil and plant water status in wine grapes under various water deficit regimes. Horttechnology **20:** 585–593

Choat B, Badel E, Burlett R, Delzon S, Cochard H, Jansen S (2016) Noninvasive measurement of vulnerability to drought induced embolism by X-ray microtomography. Plant Physiol **170:** 273–282

Choat B, Drayton WM, Brodersen C, Matthews MA, Shackel KA, Wada H, McElrone AJ (2010) Measurement of vulnerability to water stress-induced cavitation in grapevine: a comparison of four techniques applied to a long-vesseled species. Plant Cell Environ **33:** 1502–1512

Choat B, Jansen S, Brodribb TJ, Cochard H, Delzon S, Bhaskar R, Bucci SJ, Feild TS, Gleason SM, Hacke UG, et al (2012) Global convergence in the vulnerability of forests to drought. Nature **491:** 752–755

Choné X, Van Leeuwen C, Dubourdieu D, Gaudillère JP (2001) Stem water potential is a sensitive indicator of grapevine water status. Ann Bot (Lond) **87:** 477–483

Cochard H, Badel E, Herbette S, Delzon S, Choat B, Jansen S (2013) Methods for measuring plant vulnerability to cavitation: a critical review. J Exp Bot **64:** 4779–4791

Cochard H, Delzon S (2013) Hydraulic failure and repair are not routine in trees. Ann Sci **70:** 659–661

Domec JC, Scholz FG, Bucci SJ, Meinzer FC, Goldstein G, Villalobos-Vega R (2006) Diurnal and seasonal variation in root xylem embolism in neotropical savanna woody species: impact on stomatal control of plant water status. Plant Cell Environ **29:** 26–35

Donovan LA, Grise DG, West JB, Pappert RA, Alder NN, Richards JH (1999) Predawn disequilibrium between plant and soil water potentials in two desert shrubs. Oecologia **120:** 209–217

Drew MC, He CJ, Morgan PW (2000) Programmed cell death and aerenchyma formation in roots. Trends Plant Sci **5:** 123–127

Esau K (1965) Plant Anatomy, Ed 2. Wiley, New York.

Ewers BE, Oren E, Sperry JS (2000) Influence of nutrient versus water supply on hydraulic architecture and water balance in *Pinus taeda.* Plant Cell Environ **23:** 1055–1066

Frensch J, Hsiao TC (1993) Hydraulic propagation of pressure along immature and mature xylem vessels of roots of *Zea mays* measured by pressure-probe techniques. Planta **190:** 263–270

Frensch J, Steudle E (1989) Axial and radial hydraulic resistance to roots of maize (*Zea mays* L.). Plant Physiol **91:** 719–726

Gambetta GA, Fei J, Rost TL, Knipfer T, Matthews MA, Shackel KA, Walker MA, McElrone AJ (2013) Water uptake along the length of grapevine fine roots: developmental anatomy, tissue-specific aquaporin expression, and pathways of water transport. Plant Physiol **163:** 1254–1265

Gambetta GA, Manuck CM, Drucker ST, Shaghasi T, Fort K, Matthews MA, Walker MA, McElrone AJ (2012) The relationship between root hydraulics and scion vigour across *Vitis* rootstocks: what role do root aquaporins play? J Exp Bot **63:** 6445–6455

Green JJ, Dawson LA, Proctor J, Duff EI, Elston DA (2005) Fine root dynamics in a tropical rain forest is influenced by rainfall. Plant Soil **276:** 23–32

Guo D, Li H, Mitchell RJ, Han W, Hendricks JJ, Fahey TJ, Hendrick RL (2008) Fine root heterogeneity by branch order: exploring the discrepancy in root turnover estimates between minirhizotron and carbon isotopic methods. New Phytol **177:** 443–456

Hacke U, Sauter JJ (1996) Drought-induced xylem dysfunction in petioles, branches, and roots of *Populus balsamifera* L. and *Alnus glutinosa* (L.) Gaertn. Plant Physiol **111:** 413–417

Hacke UG (2000) Influence of soil porosity on water use in *Pinus taeda.* Oecologia **124:** 495–505

Hacke UG, Sperry JS, Pittermann J (2000a) Drought experience and cavitation resistance in six shrubs from the Great Basin, Utah. Basic Appl Ecol **1:** 31–41

Hendrick RL, Pregitzer KS (1996) Temporal and depth-related patterns of fine root dynamics in northern hardwood forests. J Ecol **84:** 167–176

Intrigliolo DS, Castel JR (2006) Vine and soil-based measures of water status in a Tempranillo vineyard. Vitis **45:** 157–163

Jackson RB, Mooney HA, Schulze ED (1997) A global budget for fine root biomass, surface area, and nutrient contents. Proc Natl Acad Sci USA **94:** 7362–7366

Jackson RB, Sperry JS, Dawson TE (2000) Root water uptake and transport: using physiological processes in global predictions. Trends Plant Sci **5:** 482–488PubMed

Johnson DM, Wortmann R, McCulloh KA, Jordan-Mielle L, Ward E, Warren JM, Palmroth S, Domec JC (2016) A test of the hydraulic vulnerability segmentation hypothesis in angiosperm and conifer tree species. Tree Physiol **36:** 983–993

Knipfer T, Eustis A, Brodersen C, Walker AM, McElrone AJ (2015) Grapevine species from varied native habitats exhibit differences in embolism formation/repair associated with leaf gas exchange and root pressure. Plant Cell Environ **38:** 1503–1513

Kolb KJ, Sperry JS (1999) Transport constraints on water use by the Great Basin shrub, *Artemisia tridentate.* Plant Cell Environ **22:** 925–935

Kramer PJ, Boyer JS (1995) Water relations of plant and soil (Academic Press, San Diego).

Kramer PJ, Bullock HC (1966) Seasonal variation in the proportions of suberized and unsuberized roots of trees in relation to the absorbed water. Am J Bot **53:** 200–204

Lee JE, Oliveira RS, Dawson TE, Fung I (2005) Root functioning modifies seasonal climate. Proc Natl Acad Sci USA **102:** 17576–17581

Lukac M (2012) Fine root turnover. *In* Measuring Roots. Springer, Berlin, pp 363–373.

Mainiero R, Kazda M (2006) Depth-related fine root dynamics of Fagus sylvatica during exceptional drought. For Ecol Manage **237:** 135–142

Marshall JD (1986) Drought and shade interact to cause fine-root mortality in Douglas-fir seedlings. Plant Soil **91:** 51–60

Maurel C, Boursiac Y, Luu DT, Santoni V, Shahzad Z, Verdoucq L (2015) Aquaporins in plants. Physiol Rev **95:** 1321–1358

McCormack ML, Dickie IA, Eissenstat DM, Fahey TJ, Fernandez CW, Guo D, Helmisaari HS, Hobbie EA, Iversen CM, Jackson RB, et al (2015) Redefining fine roots improves understanding of below-ground contributions to terrestrial biosphere processes. New Phytol **207:** 505–518

McCulloh KA, Johnson DM, Meinzer FC, Voelker SL, Lachenbruch B, Domec JC (2012) Hydraulic architecture of two species differing in wood density: opposing strategies in co-occurring tropical pioneer trees. Plant Cell Environ **35:** 116–125

McCulloh KA, Woodruff DR (2012) Linking stomatal sensitivity and whole-tree hydraulic architecture. Tree Physiol **32:** 369–372

McElrone AJ, Brodersen CR, Alsina MM, Drayton WM, Matthews MA, Shackel KA, Wada H, Zufferey V, Choat B (2012) Centrifuge technique consistently overestimates vulnerability to water stress-induced cavitation in grapevines as confirmed with high-resolution computed tomography. New Phytol **196:** 661–665

McElrone AJ, Choat B, Parkinson DY, MacDowell AA, Brodersen CR (2013) Using high resolution computed tomography to visualize the three dimensional structure and function of plant vasculature. J Vis Exp **74:** 10.3791/50162

McElrone AJ, Pockman WT, Martínez-Vilalta J, Jackson RB (2004) Variation in xylem structure and function in stems and roots of trees to 20 m depth. New Phytol **163:** 507–517

Nobel PS, Cui M (1992) Hydraulic conductances of the soil, the root-soil air gap, and the root: changes for desert succulents in drying soil. J Exp Bot **43:** 319–326

Nobel PS, Sanderson J (1984) Rectifier-like activities of roots of two desert succulents. J Exp Bot **35:** 727–737

North G (2004) A long drink of water: how xylem changes with depth. New Phytol **163:** 447–449

North GB, Nobel PS (1991) Changes in hydraulic conductivity and anatomy caused by drying and rewetting roots of *Agave deserti* (Agavaceae). Am J Bot **78:** 906–915

North GB, Nobel PS (1992) Drought-induced changes in hydraulic conductivity and structure in roots of *Ferocactus acanthodes* and *Opuntia ficus-indica.* New Phytol **120:** 9–19

North GB, Nobel PS (1997) Root-soil contact for the desert succulent *Agave deserti* in wet and drying soil. New Phytol **135:** 21–29

Passioura JB (1988) Water transport in and to roots. Annu Rev Plant Physiol Plant Mol Biol **39:** 245–265

Pratt RB, MacKinnon ED, Venturas MD, Crous CJ, Jacobsen AL (2015) Root resistance to cavitation is accurately measured using a centrifuge technique. Tree Physiol **35:** 185–196

Richards JH, Caldwell MM (1987) Hydraulic lift: substantial nocturnal water transport between soil layers by *Artemisia tridentata* roots. Oecologia **73:** 486–489

Schindelin J, Arganda-Carreras I, Frise E, Kaynig V, Longair M, Pietzsch T, Preibisch S, Rueden C, Saalfeld S, Schmid B, et al (2012) Fiji: an open-source platform for biological-image analysis. Nat Methods **9:** 676–682

Schulze ED, Caldwell MM, Canadell J, Mooney HA, Jackson RB, Parson D, Scholes R, Sala OE, Trimborn P (1998) Downward flux of water through roots (i.e. inverse hydraulic lift) in dry Kalahari sands. Oecologia **115:** 460–462

Sperry JS, Adler FR, Campbell GS, Comstock JP (1998) Limitation of plant water use by rhizosphere and xylem conductance: results from a model. Plant Cell Environ **21:** 347–359

Sperry JS, Ikeda T (1997) Xylem cavitation in roots and stems of Douglas-fir and white fir. Tree Physiol **17:** 275–280

Stasovski E, Peterson CA (1991) The effects of drought and subsequent rehydration on the structure and vitality of *Zea mays* seedling roots. Can J Bot **69:** 1170–1178

Steudle E, Peterson CA (1998) How does water get through roots? J Exp Bot **49:** 775–788

Tierney GL, Fahey TJ (2002) Fine root turnover in a northern hardwood forest: a direct comparison of the radiocarbon and minirhizotron methods. Can J For Res **32:** 1692–1697

Torres-Ruiz JM, Jansen S, Choat B, McElrone AJ, Cochard H, Brodribb TJ, Badel E, Burlett R, Bouche PS, Brodersen CR, et al (2015) Direct x-ray microtomography observation confirms the induction of embolism upon xylem cutting under tension. Plant Physiol **167:** 40–43

Tyree MT, Cochard H, Cruiziat P, Sinclair B, Ameglio T (1993) Drought-induced leaf shedding in walnut: evidence for vulnerability segmentation. Plant Cell Environ **16:** 879–882

Tyree MT, Ewers FW (1991) The hydraulic architecture of trees and other woody plants. New Phytol **119:** 345–360

Wheeler JK, Huggett BA, Tofte AN, Rockwell FE, Holbrook NM (2013) Cutting xylem under tension or supersaturated with gas can generate PLC and the appearance of rapid recovery from embolism. Plant Cell Environ **36:** 1938–1949

Williams LE, Araujo FJ (2002) Correlations among predawn leaf, midday leaf, and midday stem water potential and their correlations with other measures of soil and plant water status in *Vitis vinifera.* JASHS **127:** 448–454

Williams LE, Baeza P (2007) Relationships among ambient temperature and vapor pressure deficit and leaf and stem water potentials of fully irrigated, field-grown grapevines. Am J Enol Vitic **58:** 173–181

Williams LE, Baeza P, Vaughn P (2012) Midday measurements of leaf water potential and stomatal conductance are highly correlated with daily water use of Thompson Seedless grapevines. Irrig Sci **30:** 201–212

Zimmermann MH (1983) Xylem Structure and the Ascent of Sap. Springer, Berlin, Germany.